Phospholemman Modulates the Gating of Cardiac L-Type Calcium Channels

Xianming Wang,[†△] Guofeng Gao,[†△] Kai Guo,[†§] Viktor Yarotskyy,[‡] Congxin Huang,[§] Keith S. Elmslie,[‡] and Blaise Z. Peterson[†*]

[†]Department of Cellular and Molecular Physiology, and [‡]Department of Anesthesiology and Pharmacology, Pennsylvania State University College of Medicine, Hershey, Pennsylvania; and [§]Renmin Hospital, Cardiovascular Research Institute, Wuhan University, Wuhan, Hubei, People's Republic of China

ABSTRACT Ca^{2+} entry through L-type calcium channels ($Ca_V1.2$) is critical in shaping the cardiac action potential and initiating cardiac contraction. Modulation of $Ca_V1.2$ channel gating directly affects myocyte excitability and cardiac function. We have found that phospholemman (PLM), a member of the FXYD family and regulator of cardiac ion transport, coimmunoprecipitates with $Ca_V1.2$ channels from guinea pig myocytes, which suggests PLM is an endogenous modulator. Cotransfection of PLM in HEK293 cells slowed $Ca_V1.2$ current activation at voltages near the threshold for activation, slowed deactivation after long and strong depolarizing steps, enhanced the rate and magnitude of voltage-dependent inactivation (VDI), and slowed recovery from inactivation. However, Ca^{2+}-dependent inactivation was not affected. Consistent with slower channel closing, PLM significantly increased Ca^{2+} influx via $Ca_V1.2$ channels during the repolarization phase of a human cardiac action potential waveform. Our results support PLM as an endogenous regulator of $Ca_V1.2$ channel gating. The enhanced VDI induced by PLM may help protect the heart under conditions such as ischemia or tachycardia where the channels are depolarized for prolonged periods of time and could induce Ca^{2+} overload. The time and voltage-dependent slowed deactivation could represent a gating shift that helps maintain Ca^{2+} influx during the cardiac action potential waveform plateau phase.

INTRODUCTION

Voltage-gated calcium channels regulate important physiological processes such as excitation-contraction coupling, neurotransmitter release, hormone secretion, and gene expression (1). The activity of L-type calcium channels ($Ca_V1.2$) is vital for the maintenance of normal excitability and Ca^{2+} homeostasis in the heart. The dysregulation of $Ca_V1.2$ channels can lead to severe cardiac pathologies such as long QT syndrome (2–4). The modulation of $Ca_V1.2$ channels by signaling pathways and associated proteins is important for many physiological and pathophysiological processes (5–7). The gating of the α_1 subunit of the cardiac $Ca_V1.2$ channels is complex and tightly regulated (8). Drugs that target the $Ca_V1.2$ α_1 subunit are used routinely to treat cardiovascular diseases such as hypertension and angina pectoris (9,10), and α_1-associated proteins represent an important mechanism by which $Ca_V1.2$ channels are regulated (8,11,12). Thus, drugs that target the pore-forming α_1 subunit or its associated regulatory proteins have high clinical relevance.

The FXYD family of ion transport regulators was first defined based on an invariant peptide sequence, known as the FXYD motif (13). The FXYD motif is located on the N-termini of these single membrane spanning proteins and consists of five amino acids (Pro-Phe-X-Tyr-Asp). Seven members of the FXYD family (FXYD1–FXYD7) have been identified in mammals and are distributed widely in tissues that carry out fluid and solute transport (kidney, colon, breast/mammary gland, pancreas, prostate, liver, lung, and placenta), and in electrically excitable tissues (nervous system and muscle) (13,14).

FXYD1, also known as phospholemman (PLM), is localized to the sarcolemma and transverse tubules of cardiac myocytes where it regulates $[Ca^{2+}]_i$ through its interactions with Na,K-ATPase (NKA) (15–17) and the Na^+/Ca^{2+} exchanger (NCX) (18–20). As the primary pathway controlling Ca^{2+} entry into the cardiac myocyte, the observed PLM-dependent changes in $[Ca^{2+}]_i$ merit the investigation of L-type calcium channels as a possible target for PLM modulation. We present what we believe to be the first report that currents through cardiac $Ca_V1.2$ channels are modulated by PLM. Our detailed kinetic analysis demonstrates that PLM slows the activation, slows deactivation in a time and voltage dependent manner, and enhances voltage-dependent inactivation. Slowed deactivation is predicted to enhance the relative Ca^{2+} entry during the repolarization phase of the cardiac action potential. These dynamic PLM-dependent changes in $Ca_V1.2$ channel gating are expected to directly alter cell excitability, Ca^{2+} homeostasis and cardiac function.

MATERIALS AND METHODS

Coimmunoprecipitations and Western blot analysis

Antibodies

The mouse monoclonal anti-Flag M2 (Sigma-Aldrich, St. Louis, MO); rabbit polyclonal anti-$Ca_V1.2$ (Calbiochem, San Diego, CA); mouse

Submitted August 7, 2009, and accepted for publication November 18, 2009.

△Xianming Wang and Guofeng Gao contributed equally to the work.

*Correspondence: bpeterson@psu.edu

Editor: Jian Yang.

0006-3495/10/04/1149/11 $2.00

doi: 10.1016/j.bpj.2009.11.032

monoclonal anti-$Ca_V1.2$ (clone L57/46, UC Davis/National Institutes of Health NeuroMab Facility; rabbit polyclonal anti-$Ca_V2.1$ (Chemicon, Temecula, CA); rabbit polyclonal anti-PLM (C2) (a generous gift from Dr. J. Y. Cheung, Thomas Jefferson University). Pre-immune mouse IgG, pre-immune rabbit IgG, and protein A/G plus agarose were from Santa Cruz Biotech (Santa Cruz, CA). Isolation of guinea pig ventricular myocytes and subsequent coimmunoprecipitation experiments were carried out as described previously (16). Coimmunoprecipitation experiments carried out on HEK293 cell lysates were carried out as described previously (21).

Whole-cell patch-clamp electrophysiology

Whole-cell patch-clamp experiments were carried out as described previously (22). Briefly, HEK293 cells were transiently transfected with cDNAs encoding $Ca_V1.2$ (23) or $Ca_V2.1$ (GenBank No. AF055477; generously provided by Dr. Lucie Parent), the auxiliary subunits, $\alpha_2\delta$ (24) and β_1b (25), GFP (Clontech Laboratories, Mountain View, CA) and either PLM/pAdTrack or empty pAdTrack vector (both generously provided by Dr. Joseph Y. Cheung). The majority of recordings used a bath solution containing (mmol/L): 130 *N*-methyl-D-glutamine (NMG)-aspartate, 10 HEPES, 10 4-aminopyridine, 10 glucose, 1 $MgCl_2$, and 5 or 10 $CaCl_2$/$BaCl_2$ (Ba^{2+} was used unless noted otherwise). Internal solutions contained (mmol/L): 140 NMG-MeSO3, 5 EGTA, 1 $MgCl_2$, 4 Mg-ATP, and 10 HEPES. For recording $Ca_V1.2$ currents activated by a human cardiac action potential waveform, the bath solution contained (mmol/L): 140 NMG-Cl, 10 NMG-HEPES and 5 $CaCl_2$, and the internal solution contained (mmol/L): 104 NMG-Cl, 14 Creatine-PO_4, 6 $MgCl_2$, 10 NMG-HEPES, 10 NMG-EGTA, 5 Tris-ATP, 0.3 Tris-GTP. Data were acquired using either a HEKA EPC-9/2 amplifier and PULSE/PULSEFIT software (ALA Scientific Instruments, Farmingdale, NY) or an Axopatch 200A (Molecular Devices, Sunnyvale, CA) and S5 data acquisition software (Dr. Stephen Ikeda, National Institutes of Health National Institute on Alcohol Abuse and Alcoholism, Bethesda, MD). Leak and capacitive transients were corrected by −P/4 compensation and series resistance was compensated at 70%. Tail currents were sampled at 50 kHz, and filtered at 5.0 kHz. All the other currents were sampled at 20 kHz, and filtered at 3.0 kHz. Data were analyzed using Fitmaster (ALA Scientific Instruments) and Origin (Originlab, Northampton, MA) or IgorPro (WaveMetrics, Lake Oswego, OR). Results were compared using unpaired Student's *t*-test or ANOVA, as indicated, and were expressed as the mean ± SD, where $p < 0.05$ is considered significant.

RESULTS

Association of PLM with native and exogenously expressed $Ca_V1.2$ channels

Recent work showing that PLM plays an important role in regulating excitability and Ca^{2+} homeostasis in myocardium (15–19,26) prompted us to investigate the potential role PLM may play in regulating cardiac $Ca_V1.2$ channels. We carried out coimmunoprecipitation (co-IP) experiments to test for the potential association of PLM with $Ca_V1.2$ channels using solubilized membranes from guinea pig cardiac myocytes and lysates of transfected HEK293 cells (Fig. 1). As expected, $Ca_V1.2$ and PLM were observed when the solubilized membranes were subjected to Western blot analysis (Fig. 1 *A*, *lane 1*). Immunoprecipitation (IP) experiments using the anti-$Ca_V1.2$ antibodies coprecipitated PLM demonstrating an association between these proteins (Fig. 1 *A*, *lane 4*). Both $Ca_V1.2$ and PLM were absent in the insoluble and post-IP fractions (Fig. 1 *A*, *lanes 2* and *3*) and neither protein was detected in the IgG control lane (Fig. 1 *A*, *lane 5*). The plasma membrane Ca^{2+}-ATPase (PMCA) has been shown previously to have no interaction with PLM (16), was used here as a negative control (Fig. 1 *B*). As shown previously (15,16,19), we found that PLM was able to co-IP with NCX1 (Fig. 1 *C*) or NKA α_1 subunit (not shown). These results indicate that the association between $Ca_V1.2$ and PLM is specific.

We were interested determining whether PLM was capable of associating with other members of the Ca_V superfamily. Therefore, we carried out co-IP experiments using HEK293 cells transiently expressing either Flag-tagged $Ca_V1.2$ (Fig. 1 *D*), or $Ca_V2.1$ (Fig. 1 *E*) channels plus PLM. Consistent with our findings using guinea pig membranes, we found that co-IP was obtained for PLM with an anti-Flag Ab only in cells expressing both Flag-tagged $Ca_V1.2$ channels and PLM (Fig. 1D), whereas no PLM co-IP was observed when using the $Ca_V2.1$ Ab (Fig. 1 *E*). The reverse experiment of using the PLM Ab showed a co-IP of $Ca_V1.2$, but not $Ca_V2.1$ (not shown). Thus, PLM seems to specifically interact with $Ca_V1.2$ channels.

PLM specifically alters $Ca_V1.2$ channel gating

The association between PLM and $Ca_V1.2$ channels suggests the potential for gating modulation, which was examined using the HEK293 cell heterologous expression system. Whole-cell recordings from HEK293 cells expressing $Ca_V1.2$ (Fig. 2, *A–C*) or $Ca_V2.1$ (Fig. 2, *D–F*) channels in the absence (empty vector) and presence of PLM were conducted. We found that PLM slows $Ca_V1.2$ channel activation and left-shifts the activation versus voltage relationship (Fig. 2, *A* and *C*). These currents were generated by 25 ms depolarizing pulses to minimize the effect of voltage-dependent inactivation in our experiments (see below), and Ba^{2+} was used as the charge carrier to eliminate Ca^{2+}-dependent inactivation (12,27–29). The sample traces in Fig. 2 *A* show normalized currents (at −10 mV) from different cells (± PLM) to highlight the effect of PLM to slow activation. The activation versus voltage relationship measured from tail currents was left-shifted >20 mV so that the half activation voltage (V_h) changed from 25.0 to 4.1 mV with PLM and the relationship exhibited a much steeper slope factor (e-fold/23.3 vs. 12.9 mV) (Fig. 2 *C*). Consequently, at +10 mV, <40% of the channels were activated in the absence of PLM, whereas nearly 70% of the channels are activated in the presence of PLM. In contrast to $Ca_V1.2$, PLM failed to alter the activation kinetics (Fig. 2 *D*) or the voltage-dependence of activation of neuronal $Ca_V2.1$ (Fig. 2, *E* and *F*) or $Ca_V2.2$ (not shown) channels. Thus, PLM selectively associates with and modulates $Ca_V1.2$ but not $Ca_V2.1$ and $Ca_V2.2$ channels.

The voltage-dependence of PLM-induced slowed $Ca_V1.2$ channel activation was determined using currents generated during the I/V protocol (Fig. 3). The speed of activation was quantified by measuring the time required for the current

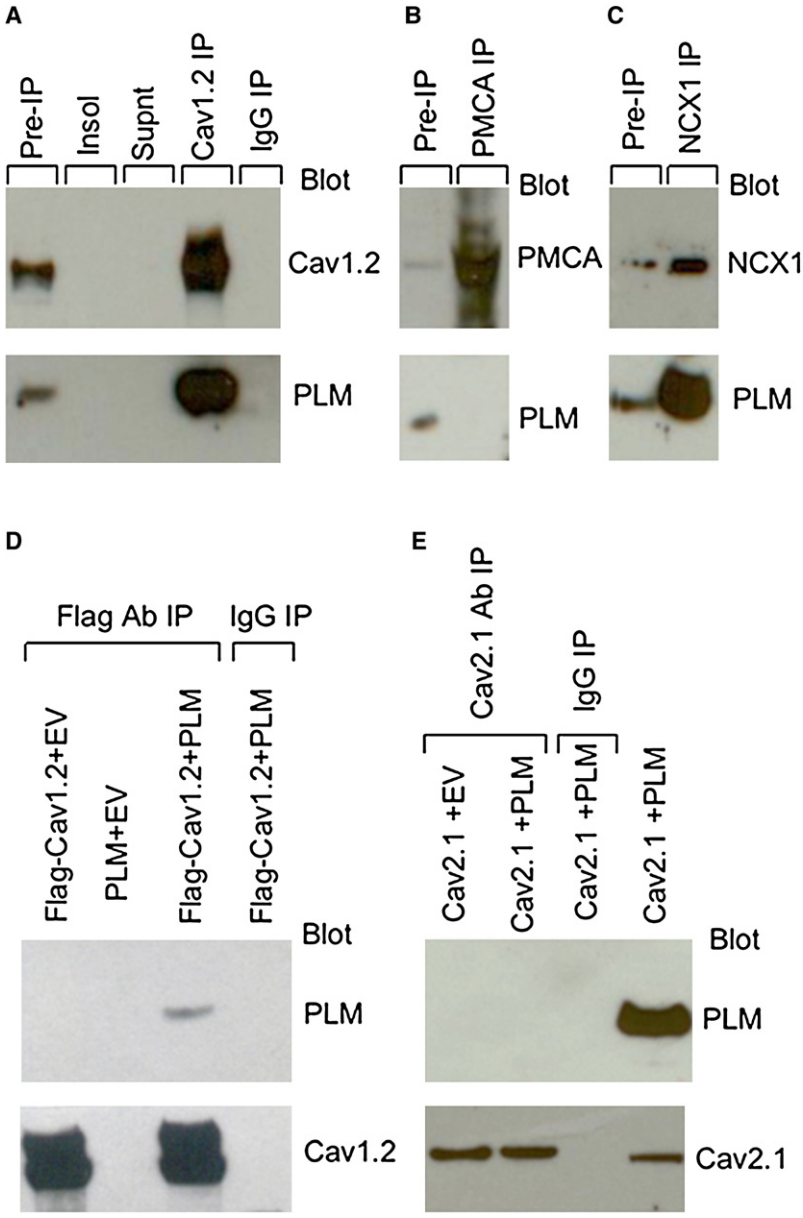

FIGURE 1 Association of PLM with native and exogenously expressed $Ca_V1.2$ channels. IP experiments were carried out on solubilized membranes derived from (*A–C*) guinea pig ventricular myocytes and (*D* and *E*) HEK 293 cell lysates using (*A*) anti-$Ca_V1.2$, (*B*, negative control) anti-PMCA antibody, (*C*, positive control) anti-NCX1, (*D*) Anti-Flag, and (*E*) anti-$Ca_V2.1$ antibodies. (*A–C*) Control lanes: Pre-IP: solubilized protein before IP; Insol: insoluble protein removed by centrifugation; Supnt: supernatant after IP; IgG: IgG control. Blots were probed with antibodies against PLM (*lower panels*) and $Ca_V1.2$, PMCA or NCX, as indicated (*upper panels*). (*D*) IP experiments carried out on lysates prepared from HEK293cells expressing $Ca_V1.2$, PLM or both as indicated using mouse monoclonal anti-Flag antibody (*lanes 1–3*) or mouse preimmune IgG (*lane 4*), followed by immunoblot analysis using antibodies against PLM (*upper panel*) and $Ca_V1.2$ (*lower panel*). (*E*) Similar to *D*, except cells were transfected with cDNAs encoding $Ca_V2.1$, PLM, or both and IP was carried out using antibodies against $Ca_V2.1$.

to increase from 10 to 90% of the peak current ($T_{10-\!-90}$). Activation was significantly slowed at hyperpolarized voltages close to the threshold for channel activation, but no significant effect was observed at voltages ≥ 0 mV (Fig. 3 *B*). It is possible that the effect of PLM on activation kinetics is voltage dependent. However, inactivation has been shown to impact the measurement of activation kinetics (30), so this interpretation is confounded by our observation that PLM expression also enhances voltage dependent inactivation at more depolarized voltages (see below).

PLM slows deactivation of $Ca_V1.2$ channels

Activation and deactivation share the same gating machinery operating in opposite directions. Thus, the PLM effect on activation may also be reflected in altered deactivation kinetics. Fig. 4 *A* shows superimposed tail currents from $Ca_V1.2$ channels $\pm$ PLM to highlight the effect of PLM on deactivation. Tail current deactivation was fit using a single exponential equation to determine the deactivation τ (τ_{Deact}). Using the I/V protocol (Fig. 2), τ_{Deact} was determined following a range of depolarizing voltages and showed an increase with voltage that was enhanced by PLM (Fig. 4 *B*). τ_{Deact} was significantly larger at all voltages for (+)PLM compared with (−)PLM. These findings suggest that the interaction of PLM with $Ca_V1.2$ channels slows channel closing.

It is well established that deactivation is slowed when $Ca_V1.2$ channels switch from mode 1 (low P_o) into mode 2 (high P_o) gating (31,32) and this gating switch is both

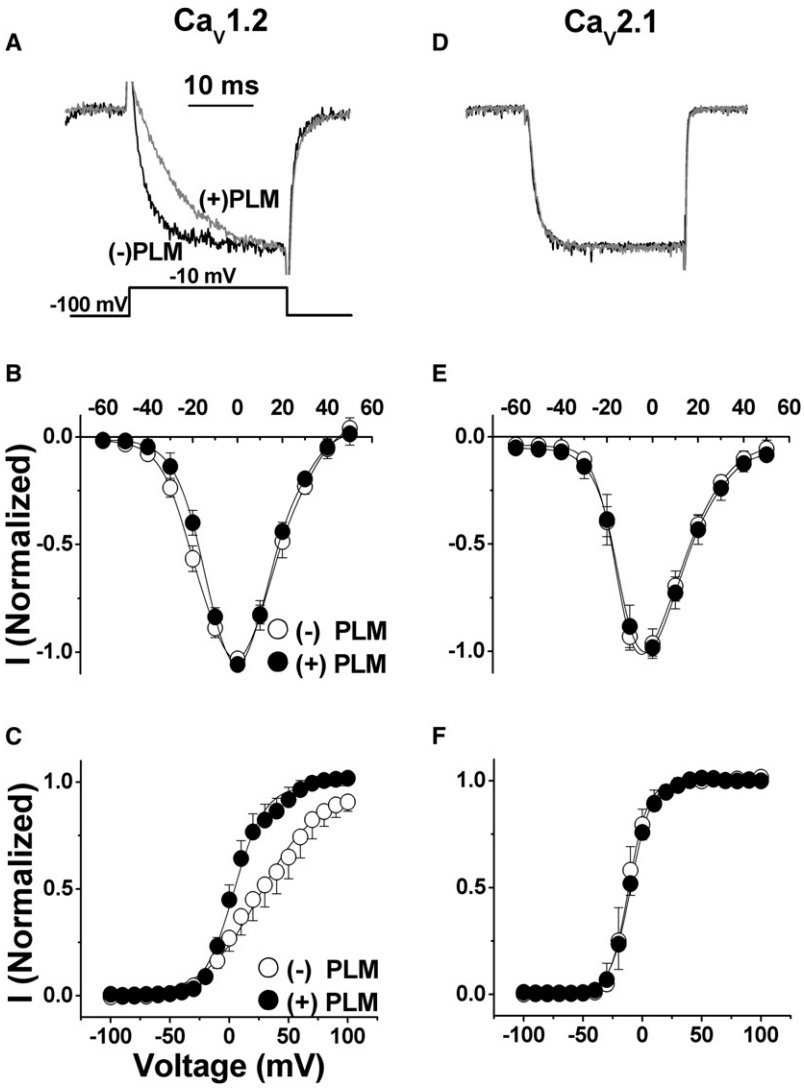

FIGURE 2 PLM alters the kinetics and voltage-dependence of $Ca_V1.2$ channel activation. Ba^{2+} currents evoked by 25 ms depolarizing steps to −10 mV in the absence ((−)PLM; *black*) and presence ((+)PLM; *gray*) for (*A*) $Ca_V1.2$ and (*D*) $Ca_V2.1$ channels were normalized to current amplitudes measured at the end of each step. Current-voltage relationships were generated ± PLM by a series of 25 ms step pulses ranging from −60 to +50 mV from a holding potential of −100 mV for (*B*) $Ca_V1.2$ and (*E*) $Ca_V2.1$. Steady-state activation curves measured from tail currents are left-shifted in the presence of PLM for (*C*) $Ca_V1.2$, but not (*F*) $Ca_V2.1$ channels. Tail currents were measured at −50 mV after a series of 25 ms step pulse 5 from −100 to +100 mV, and the data were fitted with a Boltzmann equation (*smooth lines*) to generate the half activation voltage (V_h) and slope factor (k). For $Ca_V1.2$: $V_h = 25.0 \pm 2.2$ mV and $k = 23.3 \pm 1.57$ for (−) PLM and $V_h = 4.1 \pm 0.95$ mV and $k = 12.9 \pm 0.81$ for (+)PLM. V_h and k for $Ca_V1.2$ (but not $Ca_V2.1$) currents are significantly different when measured in the absence and presence of PLM ($p < 0.05$, $n = 9$).

time- and voltage-dependent (32). Thus, if PLM enhances mode switching, the effect should depend on both step duration and voltage. We tested this prediction by measuring the time course (0–250 ms step duration) for slowed deactivation at −10; Fig. 4 *C*), +30 (Fig. 4 *D*), and +80 mV (Fig. 4 *E*). As expected, $Ca_V1.2$ currents in the absence of PLM exhibited a moderate (+80 mV) time- and voltage-dependent slowing of deactivation (increased τ_{Deact}), suggesting that some channels are transitioning from mode 1 to mode 2 gating (Fig. 4, *C–E*). In the presence of PLM, τ_{Deact} was significantly larger than (−)PLM at +80 mV for pulse durations ≥80 ms, and for +30 mV at 250 ms. It is noteworthy that changes in τ_{Deact} were not correlated with current amplitude, indicating that the PLM-induced changes do not result from voltage-clamp errors. Thus, PLM directly alters $Ca_V1.2$ gating by enhancing the voltage- and time-dependent slowing of deactivation, consistent with PLM promoting mode 2 gating. Additional single channel experiments are required to confirm this intriguing hypothesis.

PLM specifically enhances voltage-dependent inactivation of $Ca_V1.2$ channels

Examination of the records in Fig. 3 *A* shows an apparent enhancement of voltage-dependent inactivation (VDI) at the most depolarized voltage (20 mV) by PLM. This was further investigated using longer voltage steps of 300 (Fig. 5 *A*) and 1000 ms (Fig. 5 *C*) where VDI is larger and more easily measured. $Ca_V1.2$ channels exhibit little inactivation at the end of a 300 ms step in the absence of PLM, but inactivation is significantly increased in the presence of PLM. This was quantified by measuring the fraction of current remaining at the end of 300 ms (R_{300}), which was decreased significantly by PLM at voltages ≥+10 mV (Fig. 5 *B*). Longer voltage steps (1000 ms) were used to assess the impact of PLM on the speed of inactivation. Currents recorded in the presence of PLM inactivated faster (i.e., decreased inactivation τ) (Fig. 5 *E*) and the fraction of inactivating current was increased (Fig. 5, *C* and *D*),

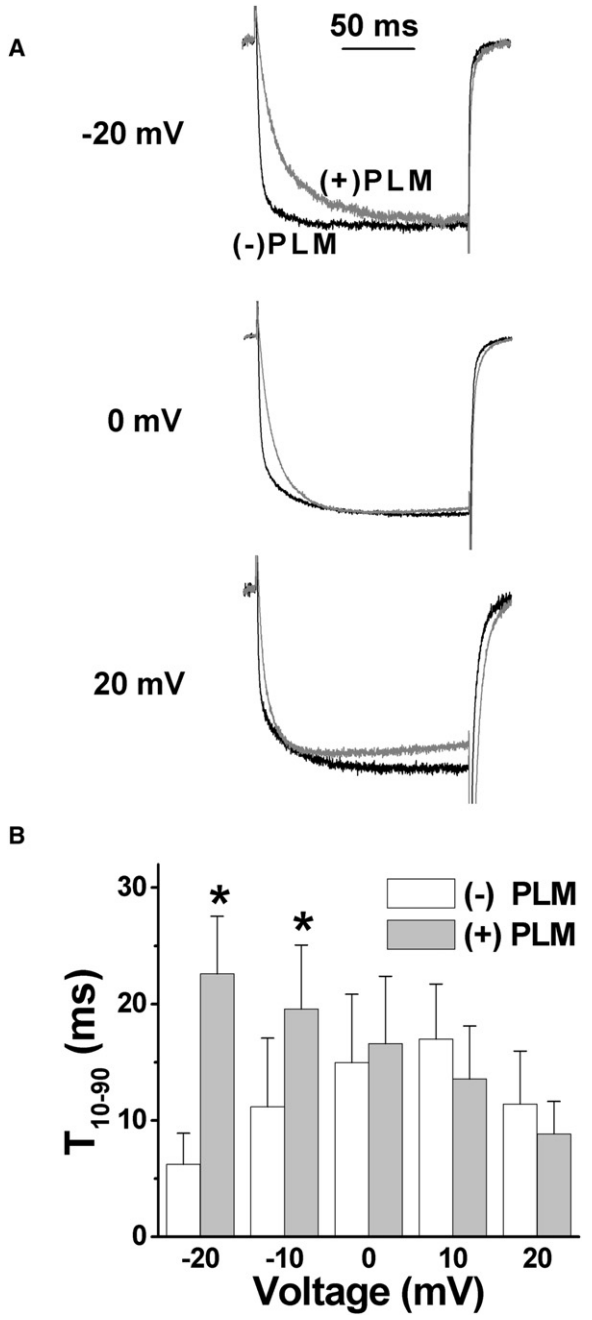

FIGURE 3 PLM slows activation of $Ca_V1.2$ channels. (*A*) Ba^{2+} currents ± PLM were generated by 150 ms voltage steps to −20, 0, and +20 mV from a holding potential of −100 mV. Slowing of activation is pronounced at −20 and 0 mV and modest at +20 mV in the presence of PLM. (*B*) The time required for channels to activate from 10 to 90% of the maximum is plotted versus step voltage ± PLM. $t_{10–90}$ is significantly increased in the presence of PLM at −20 and −10 mV ($p < 0.05$, $n = 9–12$).

suggesting that PLM may enhance the transition rate from $O \rightarrow I$ (see below). Ca^{2+} influx via $Ca_V1.2$ channels induces Ca^{2+}-dependent inactivation (CDI), but we found that PLM does not alter CDI (Fig. S1 in the Supporting Material). Therefore, it seems PLM specifically enhances the speed of VDI.

In addition to a dynamic role in shaping the cardiac action potential, inactivation is critical for establishing the number of available channels for activation and, as a result, the amount of Ca^{2+} entering the cell during each cardiac cycle (9,10). We used a standard 3-pulse protocol to determine the voltage-dependence of channel availability in the absence and presence of PLM. Peak currents were measured at 0 mV before and after 30-s steps to voltages ranging from −110 to 0 mV. The postpulse/prepulse ratio (I/I_{max}) plotted against voltage (i.e., the h_{30} curve) is depicted in Fig. 5 *F*. PLM steepens the voltage-dependence (Boltzmann slope factor) and induces a ~10 mV depolarizing shift in the h_{30} curve. Similar experiments carried out on cells expressing neuronal $Ca_V2.1$ channels in the absence and presence of PLM exhibited no change in either the half inactivation voltage or the slope factor (not shown). Thus, PLM seems to have the capacity to selectively increase the number of available $Ca_V1.2$ channels at depolarized resting membrane potentials.

PLM promotes a deep inactivated state from which recovery is slow

To better understand how PLM affects inactivation of $Ca_V1.2$ channels, we investigated the recovery from inactivation in the absence and presence of PLM. Inactivation was induced by 500 ms steps to +10 mV and quantified as the ratio of peak postpulse to prepulse currents evoked by steps to 0 mV (Fig. 6 *A*). The recovery from inactivation time course was fit by a single exponential function to determine the recovery τ (Fig. 6 *B*). $Ca_V1.2$ channels inactivated by 58% in (−)PLM and 64% in (+)PLM over the 500 ms step, and the recovery τ was nearly identical for $Ca_V1.2$ channels ± PLM (Fig. 6 *B*). However, the magnitude of recovery was significantly reduced in the presence of PLM, suggesting that PLM places the $Ca_V1.2$ channels into a deeper inactivated state from which recovery is slow. This hypothesis was tested using longer (20 s) voltage steps to place more channels into the deeper inactivated state (Fig. 6 *C*). The fraction of inactivating current resulting from 20 s depolarizing steps to +10 mV was significantly larger in the presence of PLM (98%) than was observed in the absence of PLM (87%) (Fig. 6 *D*). Interestingly, 36% of the inactivated $Ca_V1.2$ channels (−)PLM had recovered from inactivation by the first measurement point (30 ms), whereas only 12% of the channels (+)PLM had recovered by this time. This fast recovery is consistent with the recovery τ (~20 ms) measured after the 500 ms inactivating steps (Fig. 6 *B*), and further supports our hypothesis that PLM enhances the transition of channels into a deep inactivated state. $Ca_V1.2$ channels ± PLM recovered substantially more slowly after the 20-s step compared to the 500-ms step (10 s vs. 20 ms), but the recovery rates from the deep inactivated state were indistinguishable in the absence and presence of PLM (Fig. 6 *D*). Therefore, PLM increases the fraction of channels that enter the deep

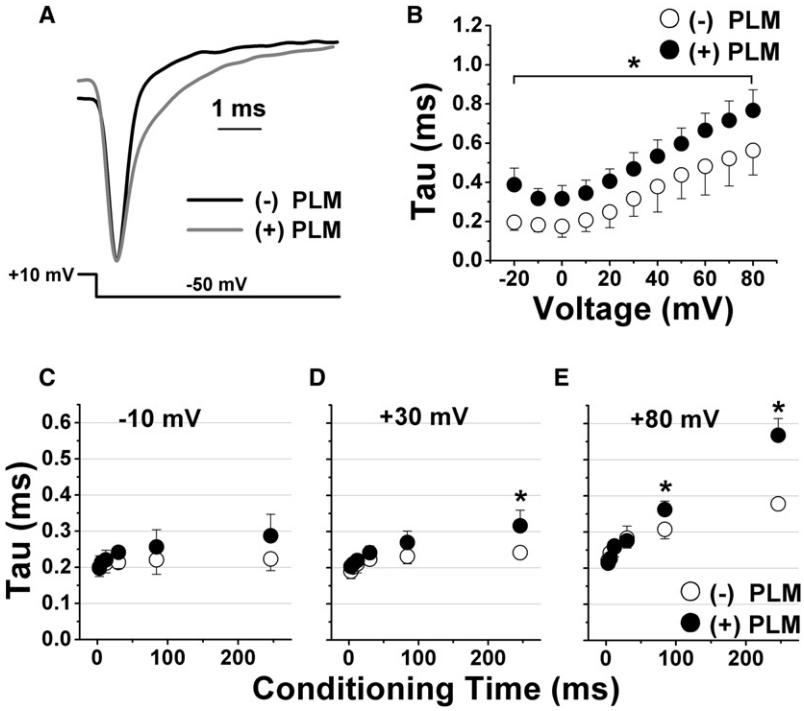

FIGURE 4 PLM slows deactivation of $Ca_V1.2$ channels. (*A*) Sample tail currents recorded in Ba^{2+} at −50 mV are shown after a 100 ms step to +10 mV. (*B*) Rate of deactivation ± PLM was evaluated using single exponential fits of tail currents recorded following voltage steps from −20 to +80 mV. Values of τ versus voltage plots indicate that PLM slows deactivation at all voltages tested (*asterisk*) (n = 5). (*C–E*) The development of slowed deactivation was evaluated using standard envelope protocol in the absence and presence of PLM. Cells were stepped to (*C*) −10, (D) +30, and (*E*) +80 mV with various durations (0–250 ms) followed by repolarizing steps to −50 mV. Tails currents were assessed using single exponential fits as described in *B* to determine voltage and time dependent values for τ. Significant differences between (−) and (+) PLM are indicated by an asterisk ($n = 4–5$).

inactivated state, but does not alter the rate at which the channels exit from that state.

PLM promotes dynamic changes in Ca^{2+} entry

PLM-induced slowing of activation and enhancement of inactivation are expected to combine to reduce Ca^{2+} entry, yet the slowing of deactivation is expected to increase Ca^{2+} entry during the cardiac action potential (4). Because PLM-induced changes in activation, inactivation, and deactivation all appear to be voltage- and time-dependent, it is likely that PLM temporally changes Ca^{2+} entry during membrane depolarization and repolarization. The effect of PLM-induced gating changes on Ca^{2+} flux can be demonstrated by comparing difference currents (Fig. 7, *A–E*) recorded in external solution with 10 mM Ca^{2+} as charge carrier. The integral of difference current provides a quantitative measure of the changes in the number of Ca^{2+} ions permeating the channels ± PLM at various time points during the depolarizing step (Fig. 7 *F*). The integral is negative at potentials <10 mV, indicating that Ca^{2+} influx is reduced during the depolarizing step in the presence of PLM, which results from slowed activation. The difference current integral becomes positive at potentials >10 mV because slowed deactivation greatly increases Ca^{2+} influx after the membrane is repolarized.

PLM increases $Ca_V1.2$ currents during the repolarization phase of the cardiac action potential

It is important to note that the changes in ionic flux elucidated by the difference currents (Fig. 7) clearly highlight important temporal aspects of PLM-induced changes in $Ca_V1.2$ channel gating. For example, slowed activation seems to play a dominant role at reducing influx during early depolarization, but slowed deactivation greatly increases flux upon repolarization. Given the time and voltage-dependent slowing of deactivation, we postulated that PLM would increase calcium entry during the repolarization phase of the cardiac action potential (cAP) after the ~200 ms plateau phase. To test this, we recorded $Ca_V1.2$ currents ± PLM generated by a human cAP waveform in 5 mM Ca^{2+} (4,33). The cAP-generated currents ± PLM exhibited a stable plateau phase and monotonic decline during repolarization. The effect of PLM on Ca^{2+} flux during the repolarization phase was assessed by normalizing currents ± PLM during the plateau phase, which showed that the duration of cAP induced-currents is increased when $Ca_V1.2$ channels are expressed with PLM (Fig. 8 *A*). This enhancement was verified by integrating the normalized current over the last 200 ms of the cAP (225–425 ms), which showed a significant increase (+)PLM. Thus, the interaction of PLM with $Ca_V1.2$ channels significantly increases Ca^{2+} influx during the repolarization phase of the cAP, which suggests that PLM plays a role in setting cAP duration and the QT interval.

DISCUSSION

We believe our findings are the first to show that PLM associates with and modulates the gating kinetics of $Ca_V1.2$ (L-type), but not $Ca_V2.1$ (P/Q-type) or $Ca_V2.2$ (N-type; not shown) channels. PLM was found to alter four important gating processes of $Ca_V1.2$ channels: 1), activation kinetics were slowed at voltages near the threshold for channel

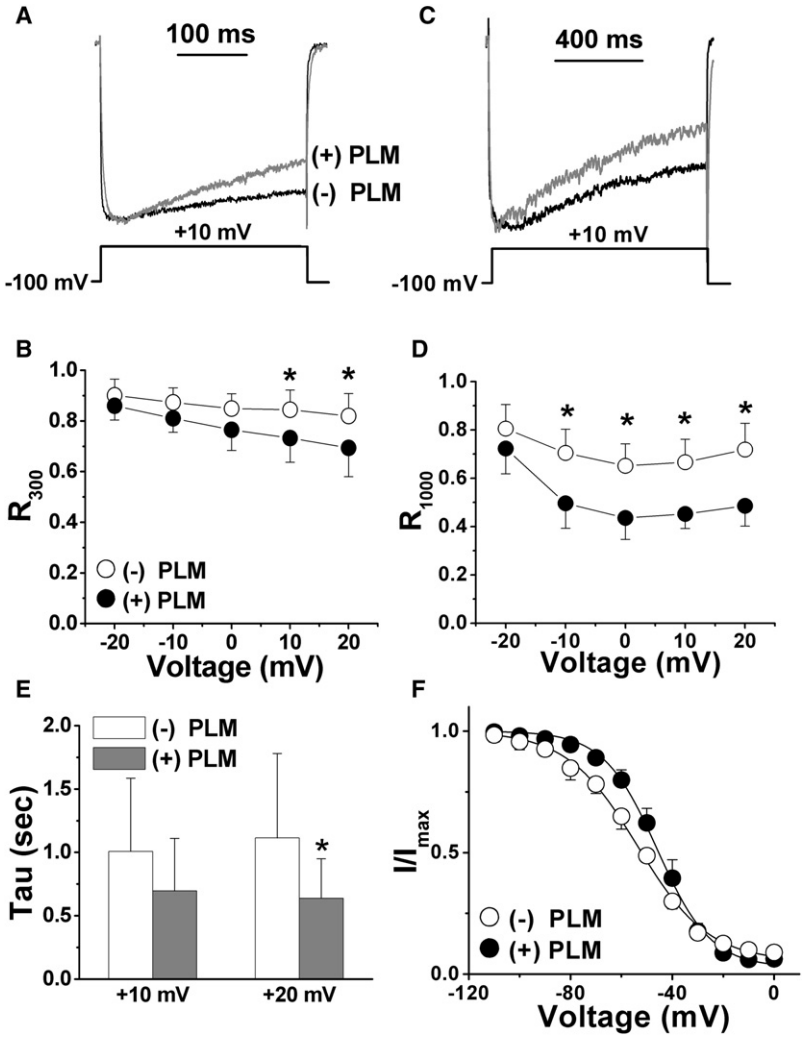

FIGURE 5 PLM enhances VDI of $Ca_V1.2$ channels. Ba^{2+} currents recorded in the absence and presence of PLM were generated by either (*A*) 300 or (*C*) 1000 ms depolarizing steps to +10 mV in 10 mM Ba^{2+}. PLM speeds the rate of inactivation (*A* and *C*) and increases the fraction of inactivating channels at 300 and 1000 ms. (*B* and *D*) The R_{300} and R_{1000} values were determined by measuring the fraction of current remaining at the end of (*B*) 300 ms (R_{300}) or (*D*) 1000 ms (R_{1000}) voltage steps. Significantly different values between (−)PLM and (+)PLM are indicated by an asterisk ($p < 0.05$). R_{300} values are averaged from 13 cells whereas 12–14 cells were used for the R_{1000} values. (*E*) Single exponential fits through currents evoked by 1000 ms voltage steps to either +10 or +20 mV indicates that PLM significantly speeds the kinetics for inactivation (τ) at +20 mV ($p < 0.05$). (*F*) A standard three-pulse protocol consisting of two 150-ms test pulses to 0 mV (pre- and postpulse) bracketing 30-s steps to voltages ranging from −110 to 0 mV was used to assess the effect PLM has on steady-state inactivation. The interval between each sweep was 80 s to allow channels to recover from previous inactivation. The postpulse/prepulse ratio (I/I_{max}) is plotted versus inactivating voltage. Single Boltzmann fits were used to determine values for V_{half} and the slope factor. In the presence of PLM, the steady-state inactivation curve is right-shifted 7.7 mV ($p < 0.05$, $n = 4$–6), and the slope factor is decreased from 13.5 ± 2.3 to 9.2 ± 2.1 ($p < 0.05$, $n = 4$–6).

activation; 2), deactivation kinetics were slowed following voltage steps comparable in magnitude and duration to that of the human cardiac action potential (cAP); 3), VDI was enhanced at potentials corresponding to the plateau phase of the cAP; and 4), an increased number of channels enter a deep inactivated state from which recovery is slow. Below, we discuss these PLM-induced changes in $Ca_V1.2$ gating in greater detail and how these PLM-dependent changes are likely to affect the cardiac action potential and contractility.

PLM-induced changes in inactivation

Recent publications have presented evidence highlighting the importance of calcium channel inactivation to cardiac function (2–4,34–39), which motivated our investigation of a potential PLM-dependent modulation of VDI. Over step depolarizations similar to the plateau phase of the cAP, PLM accelerates the rate of and increases the magnitude of VDI. The accelerated VDI at depolarized voltages (i.e., +20 mV) suggests the PLM increases the rate constant governing transition from the open (*O*) to inactivated (*I*) state, whereas the increase in VDI magnitude suggests that PLM does little to the $I \rightarrow O$ rate. This latter point is substantiated by the observation that PLM enhances the fraction of inactivating channels, which seems to be correlated with increased occupancy of a deep inactivation state from which recovery is slow ($\tau > 10$ s). We also found that the co-expression of PLM affects steady-state inactivation by shifting the half inactivation voltage ~10 mV depolarized and increasing voltage-dependence inactivation (smaller Boltzmann slope factor). The combination of right-shifted V_h and steeper voltage dependence by PLM increases the number of available channels at voltages near resting membrane potential (−80 to −50 mV). Thus, the association of PLM with $Ca_V1.2$ channels may play an important role in regulating the number of available channels under physiological and pathological conditions.

PLM-induced slowing of activation and deactivation

We observed a PLM-induced slowing of activation, but this slowing is strongly voltage-dependent and most easily

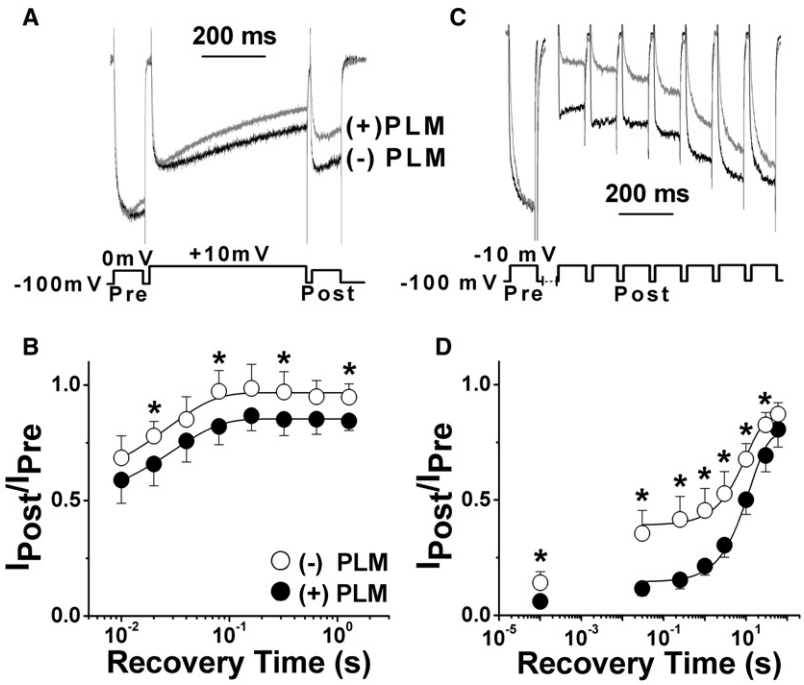

FIGURE 6 PLM promotes a deep inactivated state from which recovery is slow. (*A*) Recovery from a short inactivating pulse. Ba^{2+} currents were evoked using a three-pulse protocol with 100 ms pre- and postpulses to 0 mV bracketing a 500-ms inactivating pulse to +10 mV. The interval between the inactivation pulse and postpulse (recovery time) was increased to determine the recovery time for inactivation. The interval between sweeps was 30 s. $Ca_V1.2$ currents (±)PLM were scaled to peak prepulse current and superimposed for easier comparison. (*B*) The ratio of Ba^{2+} currents measured before and after 500 ms inactivating steps (I_{Post}/I_{Pre} ratio) is plotted versus recovery time. Smooth lines are single exponential fits: $\tau = 30.6 \pm 5.1$ and 27.3 ± 4.3 ms for (−)PLM and (+)PLM respectively ($n = 5$, not significantly different). (*C*) Recovery from a long conditioning pulse. Currents generated as described for *A* except inactivation was generated by a single 20-s step to +10 mV and the pre- and postpulse voltages were −10 mV. Recovery from inactivation was determined by a train of postpulses (shown). The 20-s inactivating pulse is not shown, but its position is indicated by a dashed line after the prepulse in pulse protocol. (*D*) The I_{Post}/I_{Pre} is plotted versus recovery time for 20-s inactivating data. Smooth lines are single exponential fits: $\tau = 10.1 \pm 1.9$ s and 12.5 ± 1.8 s for (−)PLM and (+)PLM, respectively ($n = 7$, not significantly different). Asterisks above data points indicates significant difference the fraction of recovered current between (−) and (+) PLM at each time point.

observed at potentials <0 mV. The voltage-dependence of slowed activation may result from the concurrent PLM-induced enhancement of inactivation that is more prevalent at depolarized voltages. However, during preliminary mutagenesis experiments we have identified PLM mutants that fail to enhance VDI, but still selectively slow activation at voltages <0 mV (K. Guo, X. Wang, G. Gao, C. Huang, K. S. Elmslie, B. Z. Peterson, unpublished data). This supports the idea that the PLM effect on activation is strongly voltage-dependent. Given that the $C \rightarrow O$ transition is voltage independent (4,36), the mutation findings suggest that the effect of PLM is to decrease the voltage-dependent $C \rightarrow C$ transitions, which predicts that $Ca_V1.2$ channel On-gating currents will be slowed by PLM. Those experiments are ongoing currently.

$Ca_V1.2$ channels have been shown to exhibit modal gating behavior (31,40), where the channels exist in one of three gating modes: mode 1 gating is characterized by short

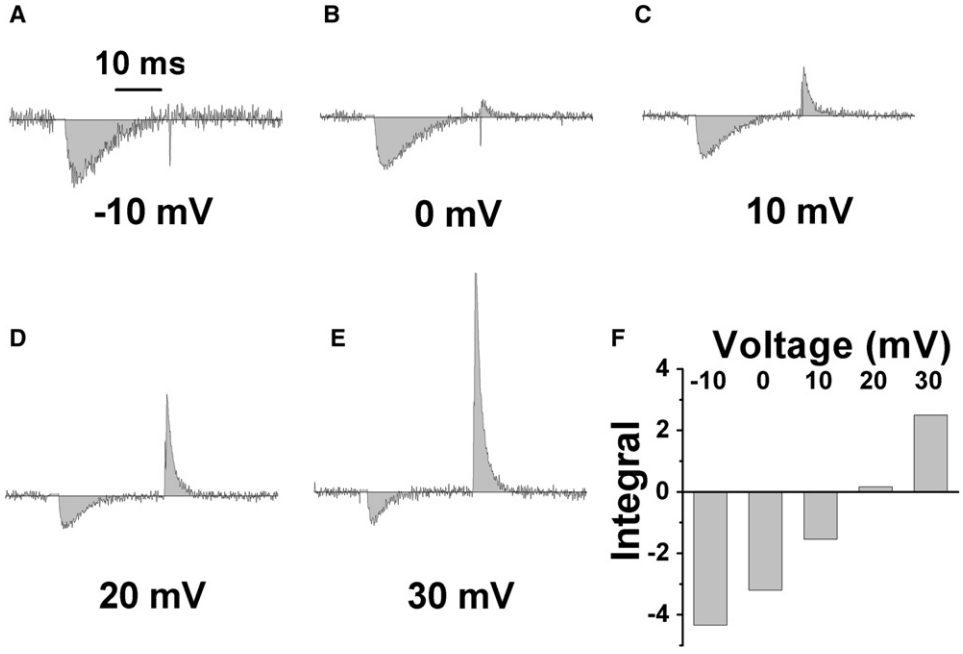

FIGURE 7 Dynamic effects of PLM on ionic flux. (*A–E*) Difference Ca^{2+} currents (10 mM Ca^{2+} as charge carrier) were calculated from averaged currents ($n = 10$–12) from cells recorded in the absence and presence of PLM for 25 ms at potentials from −10 to +30 mV. (*F*) Integrated difference currents (*gray shading*) versus step voltage were used to quantify voltage-dependent changes in Ca^{2+} flux induced by PLM.

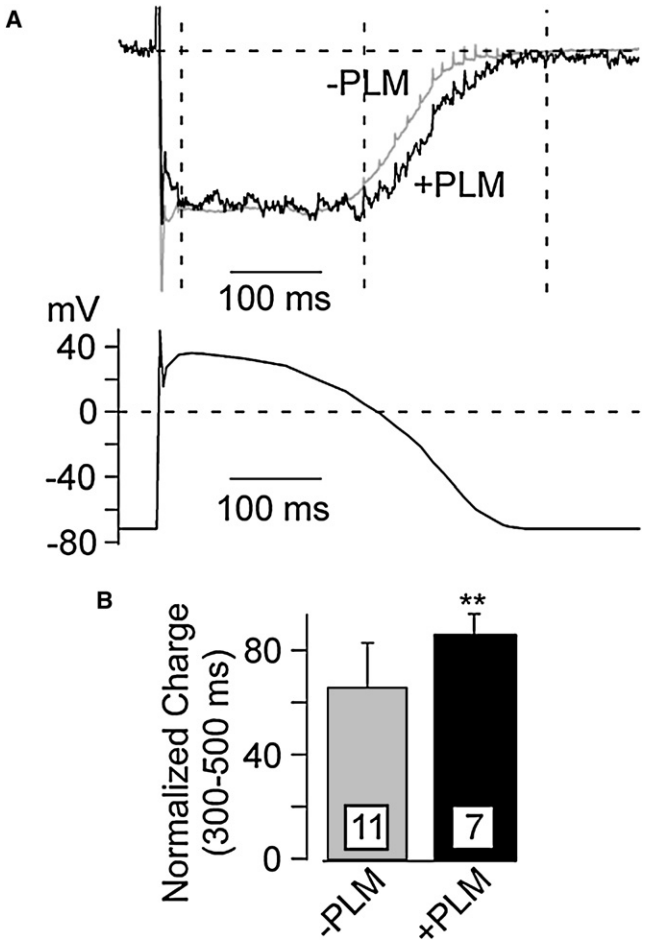

FIGURE 8 Cardiac action potential generated $Ca_V1.2$ currents are increased by PLM. (*A*) Ca^{2+} currents generated by a human cardiac action potential are superimposed from two cells in the absence (*gray trace*) or presence (*black trace*) of PLM. The currents were normalized to the plateau phase indicated by the first pair of vertical dashed lines. The second pair of vertical dashed lines corresponds to the repolarization phase of the cAP and marks the area over which the currents were integrated to determine normalized charge (*B*). (*B*) Integration of the final 200 ms of cAP-generated currents indicates that the fraction of current is increased during repolarization.

open times, low P_O and represents the predominant mode of gating; mode 2 gating occurs much less frequently and is characterized by very long open times and high P_O; and mode 0 gating is observed when the channel fails to open during a depolarizing step. Occupancy of mode 2 gating greatly slows $Ca_V1.2$ channel deactivation as measured by whole-cell tail currents (32,41,42) (5,43). Long depolarizations that mimic the cardiac action potential can induce $Ca_V1.2$ channels to switch from mode 1 into mode 2 gating (32), but these depolarizations have only modest effects to slow deactivation in HEK293 cells expressing $Ca_V1.2$ channels (−)PLM. The coexpression of PLM significantly enhances voltage-dependent slowing of deactivation so that the channels appear to more closely mimic native L-channels recorded from rat ventricular myocytes (32). Although single channel experiments are needed to confirm that PLM-enhancement of slowed deactivation results from mode switching, it seems likely that the interaction of PLM with $Ca_V1.2$ channels in cardiac myocytes regulates the voltage- and time-dependent mode switching to enhance Ca^{2+} influx.

Role of PLM in regulating excitability and contractility

The precise physiological role of PLM is not yet resolved partly because the relationships between PLM and NKA (6,15,44–47), NCX (7,48,49) and, as we report here, $Ca_V1.2$ channels, are complex, and partly because there exists some variability in the literature regarding the effect PLM expression has on contractility (7,44,45,48,50). Results from isolated myocytes suggest PLM induces a decrease in contractile strength in low Ca^{2+} and has no effect on contractility in physiological Ca^{2+} (7,48,50). However, results from whole heart suggest that PLM increases contractility in physiological Ca^{2+} (45).

Our finding that PLM modulates the gating of cardiac $Ca_V1.2$ channels further increases the complexity of the relationship between PLM expression and contractility. Changes in calcium channel gating, such as impaired VDI and slowed deactivation, profoundly affect cardiac function (2–4,34–38,51). PLM-dependent slowed deactivation seems to increase Ca^{2+} entry during the repolarization phase of the cAP and may account for the observed decrease in left ventricular pressure measured from PLM knockout mice (45). In addition, by increasing the fraction of channels occupying the deep inactivated state, PLM may help protect the heart under conditions such as ischemia or tachycardia where the channels undergo prolonged depolarization and the myocytes are vulnerable to Ca^{2+} overload.

SUPPORTING MATERIAL

A figure is available at http://www.biophysj.org/biophysj/supplemental/S0006-3495(09)01799-8.

We thank Dr. Joseph Y. Cheung for valuable suggestions and Yunhua Wang for great technical assistance.

This work was supported by grants from the National Institutes of Health (R01 HL074143 to B.Z.P.), China Scholarship Council, Chinese Scholarship Fund (to K.G.), and Pennsylvania Department of Health using Tobacco Settlement Funds (B.Z.P. and K.S.E.). The Pennsylvania Department of Health specifically disclaims responsibility for analyses, interpretations, and conclusions presented in this study.

REFERENCES

1. Hille, B. 2001. Ion Channels of Excitable Membranes. Sinauer, Sunderland, MA.
2. Splawski, I., K. W. Timothy, …, M. T. Keating. 2004. Ca(V)1.2 calcium channel dysfunction causes a multisystem disorder including arrhythmia and autism. *Cell*. 119:19–31.

3. Barrett, C. F., and R. W. Tsien. 2008. The Timothy syndrome mutation differentially affects voltage- and calcium-dependent inactivation of CaV1.2 L-type calcium channels. *Proc. Natl. Acad. Sci. USA.* 105: 2157–2162.
4. Yarotskyy, V., G. Gao, …, K. S. Elmslie. 2009. The Timothy syndrome mutation of cardiac CaV1.2 (L-type) channels: multiple altered gating mechanisms and pharmacological restoration of inactivation. *J. Physiol.* 587:551–565.
5. Buraei, Z., M. Anghelescu, and K. S. Elmslie. 2005. Slowed N-type calcium channel (CaV2.2) deactivation by the cyclin-dependent kinase inhibitor roscovitine. *Biophys. J.* 89:1681–1691.
6. Fuller, W., P. Eaton, …, M. J. Shattock. 2004. Ischemia-induced phosphorylation of phospholemman directly activates rat cardiac Na/K-ATPase. *FASEB J.* 18:197–199.
7. Mirza, M. A., X. Q. Zhang, …, J. Y. Cheung. 2004. Effects of phospholemman downregulation on contractility and $[Ca(2+)]_i$ transients in adult rat cardiac myocytes. *Am. J. Physiol. Heart Circ. Physiol.* 286: H1322–H1330.
8. Catterall, W. A., J. T. Hulme, …, W. P. Few. 2006. Regulation of sodium and calcium channels by signaling complexes. *J. Recept. Signal Transduct. Res.* 26:577–598.
9. Hockerman, G. H., B. D. Johnson, …, W. A. Catterall. 1997. Molecular determinants of high affinity phenylalkylamine block of L-type calcium channels in transmembrane segment IIIS6 and the pore region of the alpha1 subunit. *J. Biol. Chem.* 272:18759–18765.
10. Elmslie, K. S. 2004. Calcium channel blockers in the treatment of disease. *J. Neurosci. Res.* 75:733–741.
11. McDonald, T. F., S. Pelzer, …, D. J. Pelzer. 1994. Regulation and modulation of calcium channels in cardiac, skeletal, and smooth muscle cells. *Physiol. Rev.* 74:365–507.
12. Peterson, B. Z., C. D. DeMaria, …, D. T. Yue. 1999. Calmodulin is the Ca^{2+} sensor for Ca^{2+}-dependent inactivation of L-type calcium channels. *Neuron.* 22:549–558.
13. Sweadner, K. J., and E. Rael. 2000. The FXYD gene family of small ion transport regulators or channels: cDNA sequence, protein signature sequence, and expression. *Genomics.* 68:41–56.
14. Geering, K. 2006. FXYD proteins: new regulators of Na-K-ATPase. *Am. J. Physiol. Renal Physiol.* 290:F241–F250.
15. Crambert, G., M. Fuzesi, …, K. Geering. 2002. Phospholemman (FXYD1) associates with Na,K-ATPase and regulates its transport properties. *Proc. Natl. Acad. Sci. USA.* 99:11476–11481.
16. Despa, S., J. Bossuyt, …, D. M. Bers. 2005. Phospholemman-phosphorylation mediates the beta-adrenergic effects on Na/K pump function in cardiac myocytes. *Circ. Res.* 97:252–259.
17. Garty, H., and S. J. Karlish. 2006. Role of FXYD proteins in ion transport. *Annu. Rev. Physiol.* 68:431–459.
18. Zhang, X.-Q., A. Qureshi, …, J. Y. Cheung. 2003. Phospholemman modulates Na^+/Ca^{2+} exchange in adult rat cardiac myocytes. *Am. J. Physiol. Heart Circ. Physiol.* 284:H225–H233.
19. Ahlers, B. A., X.-Q. Zhang, …, J. Y. Cheung. 2005. Identification of an endogenous inhibitor of the cardiac Na^+/Ca^{2+} exchanger, phospholemman. *J. Biol. Chem.* 280:19875–19882.
20. Cheung, J. Y. 2008. Regulation of cardiac contractility: high time for FXYD. *Am. J. Physiol. Heart Circ. Physiol.* 294:H584–H585.
21. Jin, Q., W. Ding, and K. M. Mulder. 2007. Requirement for the dynein light chain km23-1 in a Smad2-dependent transforming growth factor-beta signaling pathway. *J. Biol. Chem.* 282:19122–19132.
22. Wang, X., T. A. Ponoran, …, B. Z. Peterson. 2005. Amino acid substitutions in the pore of the Ca(V)1.2 calcium channel reduce barium currents without affecting calcium currents. *Biophys. J.* 89:1731–1743.
23. Wei, X. Y., E. Perez-Reyes, …, L. Birnbaumer. 1991. Heterologous regulation of the cardiac Ca^{2+} channel alpha 1 subunit by skeletal muscle beta and gamma subunits. Implications for the structure of cardiac L-type Ca^{2+} channels. *J. Biol. Chem.* 266:21943–21947.
24. Tomlinson, W. J., A. Stea, …, T. P. Snutch. 1993. Functional properties of a neuronal class C L-type calcium channel. *Neuropharmacology.* 32:1117–1126.
25. Perez-Reyes, E., A. Castellano, …, L. Birnbaumer. 1992. Cloning and expression of a cardiac/brain beta subunit of the L-type calcium channel. *J. Biol. Chem.* 267:1792–1797.
26. Cheung, J. Y., L. I. Rothblum, …, X. Q. Zhang. 2007. Regulation of cardiac Na^+/Ca^{2+} exchanger by phospholemman. *Ann. N. Y. Acad. Sci.* 1099:119–134.
27. Zühlke, R. D., G. S. Pitt, …, H. Reuter. 1999. Calmodulin supports both inactivation and facilitation of L-type calcium channels. *Nature.* 399:159–162.
28. Lee, A., S. T. Wong, …, W. A. Catterall. 1999. Ca^{2+}/calmodulin binds to and modulates P/Q-type calcium channels. *Nature.* 399:155–159.
29. Qin, N., R. Olcese, …, L. Birnbaumer. 1999. Ca^{2+}-induced inhibition of the cardiac Ca^{2+} channel depends on calmodulin. *Proc. Natl. Acad. Sci. USA.* 96:2435–2438.
30. Elmslie, K. S., and S. W. Jones. 1994. Concentration dependence of neurotransmitter effects on calcium current kinetics in frog sympathetic neurones. *J. Physiol.* 481:35–46.
31. Hess, P., J. B. Lansman, and R. W. Tsien. 1984. Different modes of Ca channel gating behavior favored by dihydropyridine Ca agonists and antagonists. *Nature.* 311:538–544.
32. Pietrobon, D., and P. Hess. 1990. Novel mechanism of voltage-dependent gating in L-type calcium channels. *Nature.* 346:651–655.
33. Yarotskyy, V., and K. S. Elmslie. 2007. Roscovitine, a cyclin-dependent kinase inhibitor, affects several gating mechanisms to inhibit cardiac L-type (Ca(V)1.2) calcium channels. *Br. J. Pharmacol.* 152:386–395.
34. Splawski, I., K. W. Timothy, …, M. T. Keating. 2005. Severe arrhythmia disorder caused by cardiac L-type calcium channel mutations. *Proc. Natl. Acad. Sci. USA.* 102:8089–8096, discussion 8086–8088.
35. Reference deleted in proof.
36. Sicouri, S., K. W. Timothy, …, C. Antzelevitch. 2007. Cellular basis for the electrocardiographic and arrhythmic manifestations of Timothy syndrome: effects of ranolazine. *Heart Rhythm.* 4:638–647.
37. Faber, G. M., J. Silva, …, Y. Rudy. 2007. Kinetic properties of the cardiac L-type Ca^{2+} channel and its role in myocyte electrophysiology: a theoretical investigation. *Biophys. J.* 92:1522–1543.
38. Zhu, Z. I., and C. E. Clancy. 2007. L-type Ca^{2+} channel mutations and T-wave alternans: a model study. *Am. J. Physiol. Heart Circ. Physiol.* 293:H3480–H3489.
39. Findlay, I. 2002. β-Adrenergic stimulation modulates Ca^{2+}- and voltage-dependent inactivation of L-type Ca^{2+} channel currents in guinea-pig ventricular myocytes. *J. Physiol.* 541:741–751.
40. Nowycky, M. C., A. P. Fox, and R. W. Tsien. 1985. Long-opening mode of gating of neuronal calcium channels and its promotion by the dihydropyridine calcium agonist Bay K 8644. *Proc. Natl. Acad. Sci. USA.* 82:2178–2182.
41. Tsien, R. W., B. P. Bean, …, M. C. Nowycky. 1986. Mechanisms of calcium channel modulation by beta-adrenergic agents and dihydropyridine calcium agonists. *J. Mol. Cell. Cardiol.* 18:691–710.
42. Wilkens, C. M., M. Grabner, and K. G. Beam. 2001. Potentiation of the cardiac L-type Ca(2+) channel (alpha(1C)) by dihydropyridine agonist and strong depolarization occur via distinct mechanisms. *J. Gen. Physiol.* 118:495–508.
43. Marks, T. N., and S. W. Jones. 1992. Calcium currents in the A7r5 smooth muscle-derived cell line. An allosteric model for calcium channel activation and dihydropyridine agonist action. *J. Gen. Physiol.* 99:367–390.
44. Jia, L. G., C. Donnet, …, A. L. Tucker. 2005. Hypertrophy, increased ejection fraction, and reduced Na-K-ATPase activity in phospholemman-deficient mice. *Am. J. Physiol. Heart Circ. Physiol.* 288:H1982–H1988.

45. Bell, J. R., E. Kennington, …, M. J. Shattock. 2008. Characterization of the phospholemman knockout mouse heart: depressed left ventricular function with increased Na-K-ATPase activity. *Am. J. Physiol. Heart Circ. Physiol.* 294:H613–H621.

46. Reference deleted in proof.

47. Bossuyt, J., X. Ai, …, D. M. Bers. 2005. Expression and phosphorylation of the Na-pump regulatory subunit phospholemman in heart failure. *Circ. Res.* 97:558–565.

48. Song, J., X. Q. Zhang, …, J. Y. Cheung. 2002. Overexpression of phospholemman alters contractility and [Ca(2+)](i) transients in adult rat myocytes. *Am. J. Physiol. Heart Circ. Physiol.* 283:H576–H583.

49. Song, J., X. Q. Zhang, …, J. Y. Cheung. 2008. Regulation of cardiac myocyte contractility by phospholemman: Na^+/Ca^{2+} exchange versus Na^+-K^+-ATPase. *Am. J. Physiol. Heart Circ. Physiol.* 295:H1615–H1625.

50. Tucker, A. L., J. Song, …, J. Y. Cheung. 2006. Altered contractility and $[Ca2+]_i$ homeostasis in phospholemman-deficient murine myocytes: role of Na^+/Ca^{2+} exchange. *Am. J. Physiol. Heart Circ. Physiol.* 291:H2199–H2209.

51. Erxleben, C., Y. Liao, …, D. L. Armstrong. 2006. Cyclosporin and Timothy syndrome increase mode 2 gating of CaV1.2 calcium channels through aberrant phosphorylation of S6 helices. *Proc. Natl. Acad. Sci. USA.* 103:3932–3937.